

Nonequilibrium phase transitions and stationary-state solutions of a three-dimensional random-field Ising model under a time-dependent periodic external field

Yusuf Yüksel,^{*} Erol Vatansever,^{*} Ümit Akıncı, and Hamza Polat[†]
Department of Physics, Dokuz Eylül University, TR-35160 Izmir, Turkey

(Received 24 March 2012; published 16 May 2012)

Nonequilibrium behavior and dynamic phase-transition properties of a kinetic Ising model under the influence of periodically oscillating random fields have been analyzed within the framework of effective-field theory based on a decoupling approximation. A dynamic equation of motion has been solved for a simple-cubic lattice ($q = 6$) by utilizing a Glauber-type stochastic process. Amplitude of the sinusoidally oscillating magnetic field is randomly distributed on the lattice sites according to bimodal and trimodal distribution functions. For a bimodal type of amplitude distribution, it is found in the high-frequency regime that the dynamic phase diagrams of the system in the temperature versus field amplitude plane resemble the corresponding phase diagrams of the pure kinetic Ising model. Our numerical results indicate that for a bimodal distribution, both in the low- and high-frequency regimes, the dynamic phase diagrams always exhibit a coexistence region in which the stationary state (ferro or para) of the system is completely dependent on the initial conditions, whereas for a trimodal distribution, the coexistence region disappears depending on the values of the system parameters.

DOI: [10.1103/PhysRevE.85.051123](https://doi.org/10.1103/PhysRevE.85.051123)

PACS number(s): 64.60.Ht, 03.65.Vf, 75.10.Nr, 75.30.Kz

I. INTRODUCTION

The Ising model in a quenched random magnetic field [random field Ising model (RFIM)] has attracted a considerable amount of interest over the past three decades. The model, which is actually based on the local fields acting on the lattice sites that are taken to be random according to a given probability distribution, was introduced by Larkin [1] for superconductors and later generalized by Imry and Ma [2]. A lower critical dimension d_c of the RFIM has remained an unsolved mystery for many years, and now, based on the domain-wall argument of Imry and Ma [2], it is well established that a transition should exist in three and higher dimensions for finite temperature and randomness, which means that $d_c = 2$ [2–6]. On the contrary, dimensional reduction arguments [7] conclude incorrectly that the system should not have a phase transition at finite temperature in three dimensions or fewer, so $d_c = 3$ [7–11]. A great many experimental works have paid attention to the equilibrium properties of RFIM, and quite noteworthy results have been obtained. For instance, it has been shown that diluted antiferromagnets such as $\text{Fe}_x\text{Zn}_{1-x}\text{F}_2$ [12,13], $\text{Rb}_2\text{Co}_x\text{Mg}_{1-x}\text{F}_4$ [14,15], and $\text{Co}_x\text{Zn}_{1-x}\text{F}_2$ [15] in a uniform magnetic field just correspond to a ferromagnet in a random uniaxial magnetic field [16,17]. From the theoretical point of view, finite-temperature phase-transition properties of equilibrium RFIM have been studied using a wide variety of techniques, including mean-field theory (MFT) [18–22], effective-field theory (EFT) [23–27], Monte Carlo (MC) simulations [28–31], and the series expansion (SE) method [32]. Based on these theoretical works, it is well known that different random-field distributions may lead to different phase diagrams, and the presence of quenched randomness constitutes an important role in material science, since it may

induce some important macroscopic effects on the thermal and magnetic properties of real materials. On the mean-field level and for infinite-dimensional models, Schneider and Pytte [18] have shown that phase diagrams of the model exhibit only second-order phase-transition properties for a Gaussian probability distribution. Following the same methodology, Andelman [19] discussed the order of the low-temperature transition in terms of the maxima of the distribution function. Aharony [20] and Matthis [21] have introduced bimodal and trimodal distributions, respectively, and they have reported the observation of tricritical behavior. For a trimodal field distribution, Kaufman *et al.* [22] found that an ordered phase persists for arbitrarily large random fields at low temperatures. Recently, phase-transition properties of infinite-dimensional RFIMs with symmetric double- [33] and triple- [34] Gaussian random fields have also been studied by means of a replica method, and a rich variety of phase diagrams have been presented. On the other hand, based on the EFT, a tricritical point with a reentrant phase transition has been observed for three-dimensional (3D) lattices with nearest-neighbor interactions [23,24,27]. Theoretically, the situation has also been handled at zero temperature. For instance, D’Auriac and Sourlas [35] studied the RFIM on cubic lattices of various linear sizes L in three dimensions, and they found that the magnetization is discontinuous at the transition both for the Gaussian and bimodal distribution. Dhar *et al.* [36] considered the single-spin-flip dynamics of the RFIM on a Bethe lattice, and they observed that the qualitative behavior of magnetization as a function of the external field unexpectedly depends on the coordination number q of the Bethe lattice. Namely, for $q = 3$, with a Gaussian distribution of the quenched random fields, they found no jump in magnetization for any nonzero strength of disorder, whereas for $q \geq 4$ and for weak disorder, the magnetization shows a jump discontinuity as a function of the external uniform field, which disappears for a larger variance of the quenched field. Moreover, Hartmann and Nowak [37] investigated the critical behavior of the 3D RFIM with both Gaussian and bimodal distribution of random

^{*} Also at Dokuz Eylül University, Graduate School of Natural and Applied Sciences, Turkey.

[†]hamza.polat@deu.edu.tr

fields and also a 3D diluted Ising antiferromagnet in an external field. They showed that while the random-field model with a Gaussian distribution of random fields and the diluted antiferromagnet appear to be in the same universality class, the critical exponents of the random-field model with bimodal distribution of random fields were found to be significantly different. Furthermore, much effort has been devoted to determine the critical exponents of the model at zero temperature, and although the value of the heat capacity exponent α is still controversial, the values of many exponents are well established [38].

When a ferromagnetic material is subject to a periodically varying time-dependent magnetic field (kinetic Ising model), the system may not respond to the external magnetic field instantaneously, which causes interesting behaviors due to the competing time scales of the relaxation behavior of the system and periodic external magnetic field. At high temperatures and for the high amplitudes of the periodic magnetic field, the system is able to follow the external field with some delay, while this is not the case for low temperatures and small magnetic field amplitudes. This spontaneous symmetry breaking indicates the presence of a dynamic phase transition (DPT) [39], which shows itself in the dynamic order parameter (DOP), which is defined as the time average of the magnetization over a full period of the oscillating field. DPT properties of the kinetic Ising model were first observed theoretically by Tomé and Oliveira within the framework of MFT [40]. Since then, much attention has been devoted to investigate the dynamic nature of the phase transitions by means of several theoretical and experimental works. On the theoretical side, nonequilibrium phase-transition properties of the kinetic Ising model have been widely investigated using various techniques [41–51]. In addition, on the experimental side, a DPT occurring for the high-frequency magnetic fields was studied by Jiang *et al.* [52] using the surface magneto-optical Kerr-effect technique for epitaxially grown ultrathin Co films on a Cu (001) surface. For a [Co(4 Å)/Pt(7 Å)] multilayer system with strong perpendicular anisotropy, an example of DPT has been observed by Robb *et al.* [53]. They found that the experimental nonequilibrium phase diagrams strongly resemble the dynamic behavior predicted from theoretical calculations of a kinetic Ising model. It is clear from these works that there exists strong evidence of qualitative consistency between theoretical and experimental studies.

On the other hand, nonequilibrium stationary states and dynamic phase-transition properties of RFIM have not been well understood, and there exists a limited number of works in the literature [54–58]. For instance, Hausmann *et al.* [54] considered the behavior of an Ising ferromagnet under the influence of a fast switching, random external field. According to the analytical results based on MFT for the stationary state of the system, they observed a novel type of first-order phase transition which has also been verified by their extensive MC simulations. Paula *et al.* [55] determined the stationary states of the RFIM by using MFT and constructed the phase diagrams from the stationary states of the magnetization as a function of temperature and field amplitude. They found that the continuous phase transitions coincide with the equilibrium ones [20], while the first-order transitions occur at fields larger

than the corresponding values at equilibrium. In addition, they also observed that the difference between the fields at the limit of stability of the ordered phase and that of the equilibrium is maximum at zero temperature and vanishes at the tricritical point. Furthermore, Acharyya [56] studied the nonequilibrium dynamic phase transition in the two-dimensional kinetic Ising model in the presence of a randomly varying magnetic field both by MFT and MC simulations, and he discerned that in contrast to the results found in Ref. [54], the nature of the transition is always continuous. In a recent work, Crokidakis [57] performed MC simulations on cubic lattices for a nonequilibrium Ising model that stochastically evolves under the simultaneous operation of several spin-flip mechanisms where the local magnetic fields change sign randomly with time due to competing kinetics. From the numerical results, it has been predicted that there exist first-order transitions at low temperatures and large disorder strengths, which correspond to the existence of a nonequilibrium tricritical point at finite temperature. Very recently, Costabile *et al.* [58] studied the dynamical phase transitions of the kinetic Ising model in the presence of a random magnetic field by using EFT with correlations where the EFT dynamic equation has been given for the simple-cubic lattice ($q = 6$) and the dynamic order parameter has been calculated. It has been observed that the system presents ferromagnetic and paramagnetic states for low and high temperatures, respectively. Apart from this, they have predicted a nonequilibrium tricritical point in a phase diagram in the temperature versus applied field amplitude plane. They have also compared the results with the equilibrium phase diagram [23,24], where only the first-order line is different. In the theoretical works mentioned above, the random-field effects have been taken into account either by a given probability distribution function (random in space), namely a bimodal distribution, or by generating a new configuration of random fields uniformly at each time step (random in time).

Recently, some of us have investigated the static properties of the RFIM for continuous field distributions by introducing an EFT method in which an approach has been made to take into consideration the multisite as well as the single-site correlations between different spins [27], which provided a treatment beyond the conventional MFT and EFT in a quantitative manner. However, before attempting to adopt the consideration of multisite correlations to the kinetic RFIM model, it would be beneficial to shed some light on critical properties of the system by utilizing an uncomplicated tool. Hence, in the present paper, we have studied dynamic phase transitions and stationary states of the RFIM driven by a periodically varying time-dependent magnetic field on a simple-cubic lattice in which the multisite correlations between different sites that emerge when expanding the identities are treated by introducing a decoupling procedure that is quite superior to conventional MFT. The amplitude of the applied magnetic field is sampled from both bimodal and trimodal probability distributions, which are relevant to diluted antiferromagnets in a uniform field [22]. For this purpose, we organized the paper as follows: In Sec. II, we briefly present the formulations. The results and discussions are summarized in Sec. III, and finally Sec. IV contains our conclusions.

II. FORMULATION

We consider a three-dimensional Ising ferromagnet ($J > 0$) defined on a simple-cubic lattice with a time-dependent external magnetic field. The time-dependent Hamiltonian describing our model is

$$\mathcal{H} = -J \sum_{\langle ij \rangle} S_i S_j - \sum_i H_i(t) S_i, \quad (1)$$

where the first term is a summation over the nearest-neighbor spins with $S_i = \pm 1$, and $H_i(t)$ is a time-dependent external oscillating magnetic field which is given by

$$H_i(t) = H_{0i} \cos(\omega t), \quad (2)$$

where H_{0i} is the amplitude of the external magnetic field acting on the site i , and ω denotes the angular frequency of the oscillating external field. The amplitude of the field is distributed according to a given probability distribution function. The present study deals with a trimodal field distribution which has a form

$$P(H_{0i}) = p \delta(H_{0i}) + \left(\frac{1-p}{2} \right) [\delta(H_{0i} - H_0) + \delta(H_{0i} + H_0)]. \quad (3)$$

In order to describe the dynamical evolution of the system, we follow a Glauber-type stochastic process [59]. The dynamical equation of motion can be obtained by using the master equation as follows:

$$\tau \frac{d\langle S_i \rangle}{dt} = -\langle S_i \rangle + \left\langle \tanh \left[\frac{E_i + H_i(t)}{k_B T} \right] \right\rangle, \quad (4)$$

where τ is the transition rate per unit time, $E_i = J \sum_j S_j$ is the local field acting on the lattice site i , and k_B and T denote the Boltzmann constant and temperature, respectively.

In Eq. (4), we set τ to unity. If we apply the differential operator technique [60,61] in Eq. (4) by taking into account the random configurational averages, we get

$$\frac{dm}{dt} = -m + \left\langle \left\langle \prod_{j=1}^{q-6} \cosh(J\nabla) + S_i \sinh(J\nabla) \right\rangle \right\rangle_r F(x)|_{x=0}, \quad (5)$$

where $m = \langle \langle S_i \rangle \rangle_r$ represents the average magnetization, $\nabla = \partial/\partial x$ is a differential operator, q is the coordination number of the lattice, and the inner $\langle \dots \rangle$ and the outer $\langle \dots \rangle_r$ brackets represent the thermal and configurational averages, respectively. Actually, the representation $\langle \langle S_i \rangle \rangle_r$ is a conventional notation, and the lattice sites are independent of the random configurations of the local magnetic fields. In fact, the disorder averaging procedure is relevant to the function $F(x)$ in Eq. (5), which explicitly includes the magnetic field term. The function $F(x)$ in Eq. (5) is then defined by

$$F(x) = \int dH_{0i} P(H_{0i}) \tanh \left[\frac{x + H_i(t)}{k_B T} \right]. \quad (6)$$

Hence, in order to perform the disorder-averaging procedure, one should evaluate the numerical integration defined in Eq. (6) at each time step t for given Hamiltonian parameters and temperature. When the right-hand side of Eq. (5) is expanded, the multispin correlation functions appear. The simplest

approximation, and one of the most frequently adopted, is to decouple these correlations according to

$$\langle \langle S_i S_j \dots S_l \rangle \rangle_r \cong \langle \langle S_i \rangle \rangle_r \langle \langle S_j \rangle \rangle_r \dots \langle \langle S_l \rangle \rangle_r \quad (7)$$

for $i \neq j \neq \dots \neq l$ [62]. If we expand the right-hand side of Eq. (5) within the help of Eq. (7), then we obtain the dynamical equation of motion as follows:

$$\frac{dm}{dt} = -m + \sum_{j=0}^{q=6} \Lambda_j m^j. \quad (8)$$

The coefficients in Eq. (8) are defined as

$$\Lambda_j = \frac{1}{2^q} \sum_{r=0}^{q-j} \sum_{s=0}^j \binom{q-j}{r} \binom{j}{s} (-1)^s \times \exp[(q-2r-2s)J\nabla] F(x)|_{x=0}, \quad j = 0, 1, \dots, q. \quad (9)$$

These coefficients can be calculated by employing the mathematical relation $\exp(\alpha\nabla)F(x) = F(x + \alpha)$ after evaluating Eq. (6) numerically. Equation (8) can be regarded as a kind of initial-value problem and the solution can be easily found by benefiting from the initial value of the average order parameter m_0 , and by using the fourth-order Runge-Kutta method (RK-4). For selected values of the Hamiltonian parameters and temperature, the time dependence of magnetization converges to a finite value after some iterations, i.e., the solutions have the property $m(t) = m(t + 2\pi/\omega)$ for the arbitrary initial value of the magnetization (m_0). Thus, by obtaining this convergent region after some transient steps (which depends on Hamiltonian parameters and the temperature), the DOP, which is the time average of the magnetization over a full cycle of the oscillating magnetic field, can be calculated from

$$Q = \frac{\omega}{2\pi} \oint m(t) dt, \quad (10)$$

where $m(t)$ is a stable and periodic function which can be one of the two types, according to whether it has the following property or not [40]:

$$m(t) = -m(t + \pi/\omega). \quad (11)$$

A solution satisfying Eq. (11) is called a symmetric solution, which corresponds to a paramagnetic (P) phase where the magnetization oscillates around zero; the solution which does not ensure Eq. (11) is called a nonsymmetric solution, and it corresponds to a ferromagnetic (F) phase where the magnetization oscillates around a nonzero value. In these two cases, the observed behavior of the magnetization is independent of the choice of the initial value of magnetization. On the other hand, in contrast to the equilibrium RFIM, there exist coexistence regions (F + P phases) in the phase diagrams in temperature versus field amplitude plane where the stationary state of the nonequilibrium RFIM problem depends on the initial value m_0 of the time-dependent magnetization. Furthermore, it is not possible to obtain the free energy for kinetic models in the presence of time-dependent external fields. Hence, in order to determine the type of dynamic phase transition (first or second order), it is convenient to check the temperature dependence of DOP. Namely, if the DOP decreases continuously to zero in the vicinity of critical temperature, this transition is classified

as second order, whereas if it vanishes discontinuously, then the transition is assumed to be first order.

III. RESULTS AND DISCUSSION

In this section, we discuss how the random fields affect the phase diagrams of the kinetic Ising model. Also, in order to clarify the type of dynamic phase transitions in the system, we give the temperature dependence of the dynamic order parameter.

A. Nonequilibrium phase diagrams of the kinetic model: Pure case

In order to provide a testing ground for our calculations, we have primarily studied the dynamic phase diagrams of the kinetic Ising model under an oscillating magnetic field where the amplitude of the externally applied field was taken as a uniformly constant value. This model defines nonequilibrium properties of the pure system and has been examined previously within the framework of EFT [49,51]. In these works, the authors investigated the phase diagrams of the system in a $(k_B T_c/qJ - H_0/qJ)$ plane, where q is the coordination number of the lattice. From these works, we see that, for the oscillation frequency values $\omega = 0.5$ and 1.0 , the location of the dynamic tricritical (DTC) point was identified imprecisely. Hence, in order to compare our results with those found in Refs. [49,51], we depict the phase diagrams in Fig. 1 in the same plane. It is clear from Fig. 1 that our numerical values of the DTC point coordinates for $\omega = 0.5$ and 1.0 agree qualitatively well with Ref. [51], whereas they are qualitatively and quantitatively quite different from those obtained in Ref. [49]. It is not possible to compare our numerical results for DTC point coordinates as a function of ω in the $(k_B T_c/qJ - h_0/qJ)$ plane with those obtained in Ref. [51] since they did not report numerical values. On the other hand, in Ref. [49], numerical results for DTC points

are reported as $(0.406, 0.473)$ and $(0.402, 0.608)$ for frequency values $\omega = 0.5$ and 1.0 , respectively, which are quite different from our results $(0.192, 0.630)$ for $\omega = 0.5$ and $(0.233, 0.688)$ for $\omega = 1.0$. The discrepancy is probably due to the fact that in Ref. [49], an insufficient number of data points was used to construct the phase diagrams of the system. In addition, another conflict between the results obtained in the present work and those obtained in Ref. [49] is that the F + P phase, which is located in the low-temperature and large-amplitude region in Fig. 1, is not reported in Ref. [49].

B. Nonequilibrium phase diagrams of the RFIM for a bimodal distribution

The distribution function given in Eq. (3) corresponds to a bimodal field distribution for $p = 0$ where the amplitude of the oscillating field can be either $+H_0$ or $-H_0$ with equal probability. In this case, the system can be thought of as a spin system under the influence of two oscillating external field sources. In Refs. [55,58], a similar model has been studied within MFT and EFT, respectively, where the authors did not consider any oscillating external magnetic field. The main conclusion of those studies was that the dynamic second-order phase-transition lines in the $(k_B T_c/J - H_0/J)$ plane coincide with the equilibrium counterparts [20,23,24], whereas the maximum and minimum differences between the dynamic and equilibrium first-order phase transition lines were observed at the zero temperature and at the tricritical point, respectively. However, as seen in Figs. 2(a) and 2(b), if the external magnetic field has an oscillatory character with an amplitude which is applied at random, then a completely different situation arises. Namely, the second-order phase-transition fields of nonequilibrium RFIM with oscillating random external fields are greater than those obtained for the static RFIM [23,24]. We should note that the consideration of multisite correlations in the static RFIM [27] produces qualitatively similar phase diagrams to those obtained in Refs. [23,24], where the authors neglected these higher-order correlations by using the approximation given in Eq. (7). On the other hand, according to the dynamic phase diagrams shown in Figs. 2(a) and 2(b), the system may exhibit F phase for low-field amplitude values even at high temperatures. As the field sources are switched on, the spins tend to point up or down randomly by aligning with the periodically oscillating local fields acting on the lattice sites. For small H_0/J values, the nearest-neighbor bonds are dominant against the periodic local fields to allow all spins to order. Hence, a relatively large amount of thermal energy is needed to observe a dynamic phase transition in the system, due to the response of the spins to the external magnetic field. As H_0/J increases, then the ferromagnetic exchange interaction loses its dominance against the external field amplitude and it becomes possible to observe a dynamic phase transition at lower temperatures. Hence, the system is able to follow the external field with some delay. In addition, as the oscillation frequency ω increases, the DTC point depresses and the F + P phase region gets narrower. In Figs. 2(c) and 2(d), variations of DTC point coordinates H_0^t/J and $k_B T^t/J$ with respect to the frequency ω are plotted, respectively. As seen in this figure, H_0^t/J grows whereas $k_B T^t/J$ decays with increasing ω , and these values saturate at $H_0^t/J = 4.512$ and

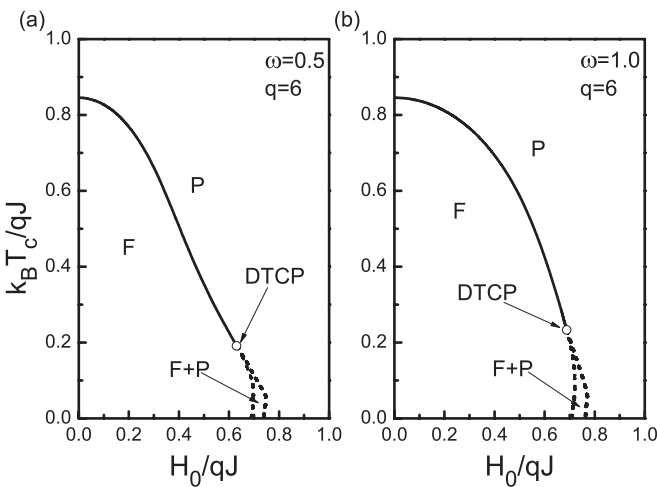


FIG. 1. Dynamic phase diagram of the pure kinetic Ising model in the $(k_B T/qJ - H_0/qJ)$ plane for oscillation frequency values $\omega = 0.5$ (a) and $\omega = 1.0$ (b), for comparison with Refs. [49,51]. Solid (dashed) lines correspond to second- (first-) order phase transitions, and hollow circles represent dynamic tricritical points (denoted as DTCP).

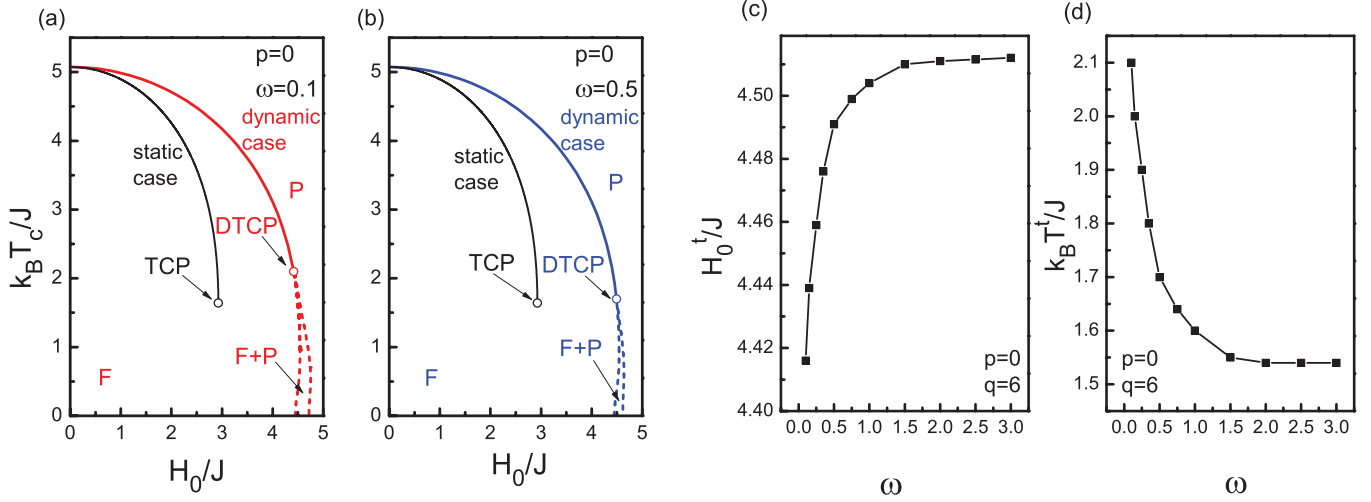


FIG. 2. (Color online) Phase diagrams of the kinetic RFIM in the $(k_B T_c/J - H_0/J)$ plane for a bimodal distribution with (a) $\omega = 0.1$ and (b) 0.5 , in comparison with the static model [23,24]. Solid (dashed) lines correspond to second- (first-) order phase transitions, and hollow circles represent tricritical points. The right panel shows the variation of the dynamic tricritical point coordinates (c) H_0^t/J and (d) $k_B T^t/J$ as a function of frequency ω .

$k_B T^t/J = 1.54$. This means that the coexistence region in the phase diagrams gets narrower but does not disappear with increasing ω . In other words, for sufficiently high frequencies, both the location of the DTC point and the area of the F + P region become independent of oscillation frequency of the external field. We also note that the F region is always independent of frequency for the whole range of ω .

In Fig. 3, we show the temperature dependence of the dynamic order parameter Q as a function of the oscillation frequency ω corresponding to the phase diagrams depicted in Fig. 2. As we mentioned before, increasing or decreasing frequency values do not affect the area of the F region. Namely, for a fixed H_0/J value, the system always undergoes a dynamic

phase transition on the F-P phase boundary line, and the critical temperature value is independent of ω . This situation is independent of the selection of the initial magnetization for $H_0/J < H_0^t/J$, whereas it is valid for $H_0/J > H_0^t/J$ only if one starts with an initial condition $m_0 = 0$. As is clearly seen in Fig. 3(a), all curves coincide with each other for $H_0/J = 2.0$. The inset in Fig. 3(a) shows the average magnetization $m(t)$ as a function of time t at $k_B T/J = 4.0$ and for $\omega = 0.1, 0.3$, and 0.5 , where we see that the $m(t)$ curve oscillates with smaller amplitude as ω increases, but the average value, i.e., DOP (Q) over a complete cycle of the magnetic field, does not change. On the other hand, as shown in Fig. 3(b), for sufficiently strong amplitudes of the external field, such as $H_0/J = 4.0$, DOP versus temperature curves exhibit different characteristics with increasing frequency, although the critical temperature does not change, and interestingly, for sufficiently high-frequency values such as $\omega \geq 0.5$, DOP curves resemble those of the pure kinetic Ising model driven by a periodic external field with the high oscillation frequency.

In Fig. 4, dynamic phase diagrams of the system are depicted for a wide range of oscillation frequency values. In this figure, we observe that the DTC point depresses for a while and the area of the coexistence region in the phase diagrams gets slightly narrower and then remains unchanged with increasing frequency values. The low-frequency phase diagrams of the system are found to be completely different from those of the pure kinetic Ising model [51], whereas for the high-frequency regime, dynamic phase diagrams of the system are exactly identical to those of the pure case. These observations originate from the symmetry of the random-field distribution. Namely, for a bimodal field distribution, we have two oscillating magnetic field sources. Initially, half of the lattice sites are under the influence of a periodically oscillating field (source 1) with an amplitude H_0/J , and the remaining spins on the other half of the lattice are influenced by an oscillating external field with an amplitude $-H_0/J$ (source 2). As time progresses, due to the sinusoidal

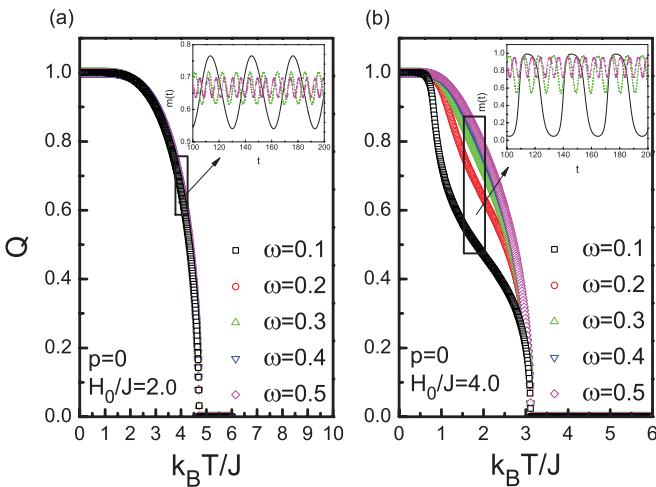


FIG. 3. (Color online) Temperature dependence of the dynamic order parameter Q as a function of frequency ω for (a) $H_0/J = 2.0$ and (b) 4.0 . Insets in both panels show the time variation of the average magnetization $m(t)$ at $k_B T/J = 4.0$ (left) and 1.75 (right), respectively, where the oscillation amplitude of the magnetization decreases as ω increases from 0.1 to 0.5 .

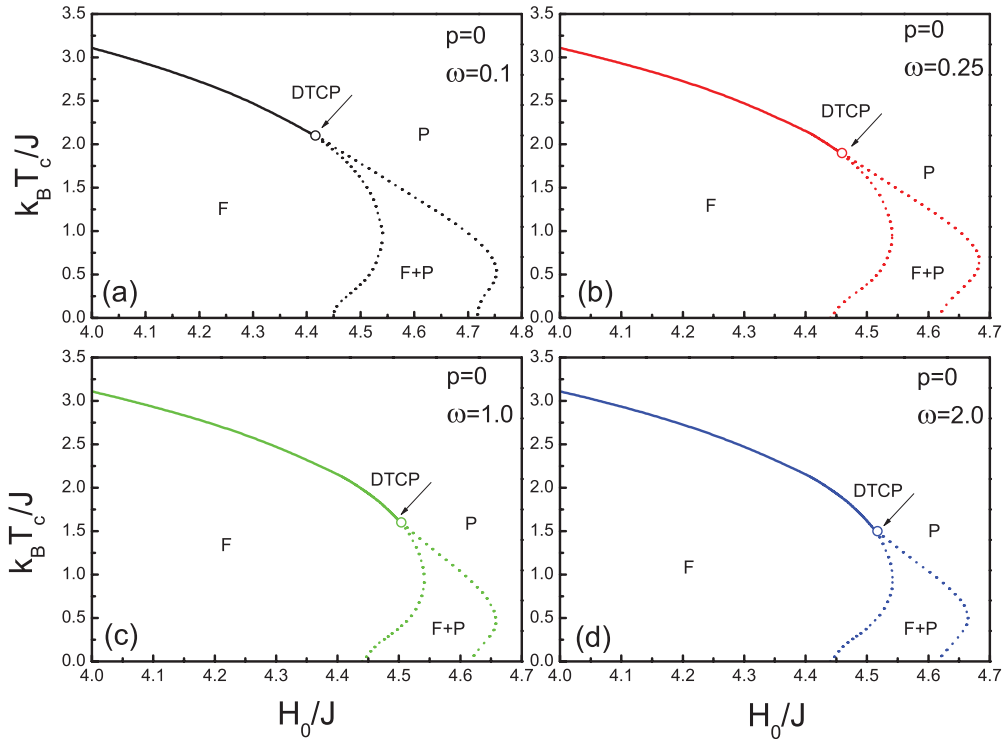


FIG. 4. (Color online) Dynamic phase diagrams of the system in a $(k_B T_c / J - H_0 / J)$ plane for a bimodal distribution with some selected values of frequency (a) $\omega = 0.1$, (b) $\omega = 0.25$, (c) $\omega = 1.0$, and (d) $\omega = 2.0$. The solid (dashed) lines correspond to second- (first-) order phase transitions, and hollow circles represent dynamic tricritical points.

form of the periodic fields, magnetic field sources acting on the lattice sites change their sign instantaneously at the end of one-half of the oscillation period. Consequently, the presence of a phase difference between source 1 and source 2 stimulates some unusual effects on the system. Furthermore, for sufficiently high frequencies of the oscillating external fields, the relaxation time of the system becomes greater than the oscillation period of the external field. As a result, source-1 and source-2 fields receive identical responses from

the system, which perceives the field sources as a single oscillatory field source, hence the dynamic phase diagrams of the system resemble the high-frequency phase diagrams of the corresponding pure model. We may also note that F + P regions in the $(k_B T_c / J - H_0 / J)$ phase diagrams always exist for the whole range of frequency values.

In Fig. 5, we represent some examples of typical DOP versus temperature profiles corresponding to the phase diagrams shown in Fig. 4 with $\omega = 1.0$. Namely, the system always undergoes a second-order dynamic phase transition for $H_0 / J = 4.4$. In this case, the dynamic nature of the phase transition and the stationary state of the system are independent of the initial magnetization m_0 . On the other hand, two successive first-order dynamic phase transitions (i.e., a first-order reentrant phenomena) occur at the value $H_0 / J = 4.52$ with the initial condition $m_0 = 0.0$. In addition, for $H_0 / J = 4.6$ with $m_0 = 1.0$, the DOP curve exhibits a discontinuous jump at a phase-transition temperature, which suggests the existence of a first-order transition in the system. For the latter two examples, the dynamic nature of the phase transition and the stationary state of the system strictly depend on the initial magnetization.

C. Nonequilibrium phase diagrams of the RFIM for a trimodal distribution

For a trimodal field distribution of magnetic fields defined in Eq. (3), we plot the dynamic phase diagrams of the system in a $(k_B T_c / J - H_0 / J)$ plane in Fig. 6 for $\omega = 0.5$ and with some selected values of disorder parameter p . This distribution corresponds physically to a diluted bimodal distribution in

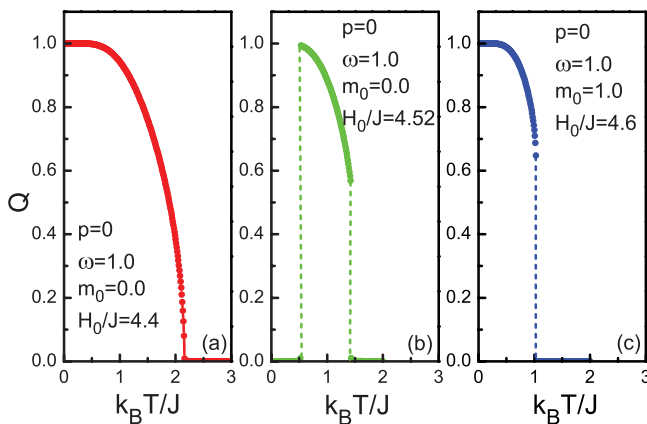


FIG. 5. (Color online) Variation of the dynamic order parameter Q as a function of the temperature for $\omega = 1.0$ with some selected values of initial magnetization and external field amplitude: (a) $m_0 = 0.0$ and $H_0 / J = 4.4$, (b) $m_0 = 0.0$ and $H_0 / J = 4.52$, and (c) $m_0 = 1.0$ and $H_0 / J = 4.6$. The dashed lines correspond to the first-order phase transitions.

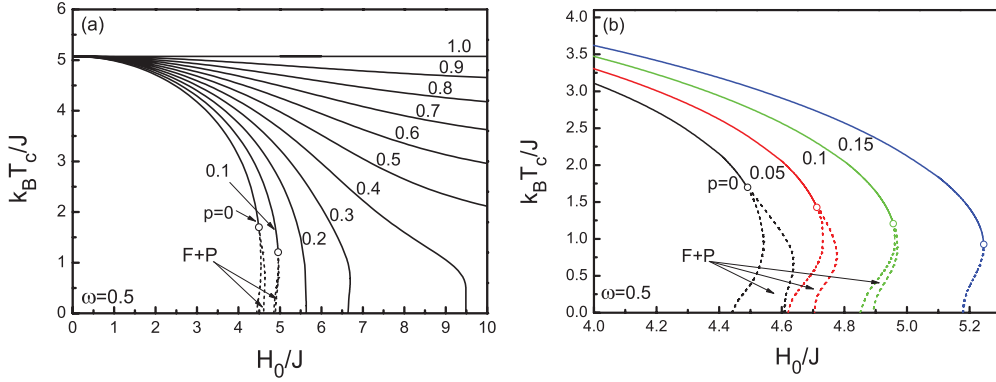


FIG. 6. (Color online) Dynamic phase diagrams of the system in a $(k_B T_c/J - H_0/J)$ plane for a trimodal distribution of random fields with $\omega = 0.5$ and for some selected values of p . The solid (dashed) lines correspond to second- (first-) order phase transitions, and hollow circles represent dynamic tricritical points.

which a fraction p of the lattice sites are not exposed to the oscillating external field [21]. As shown in Fig. 6(a), the system exhibits DTC behavior for a relatively narrow range of p . The temperature coordinate $k_B T_c/J$ of the DTC point decreases as p increases, whereas the field amplitude part H_0^t/J increases, and consequently the DTC point depresses to zero at a certain value of p . After the destruction of the DTC point, all dynamic phase-transition processes are found to be second order. We also note that at zero temperature, there exists a critical value $p^* = 0.53$ below which the system exhibits a dynamic phase transition at a critical magnetic field. This value of p^* is independent of ω . In other words, as p increases, the fraction of the spins which are subjected to no magnetic field increases. Consequently, for $p > p^*$ this fraction is sufficient for the system to form an infinite cluster in which the spins can order ferromagnetically at low temperatures for arbitrarily large values of the random amplitude of the oscillating magnetic field. Hence, the ferromagnetic region extends to large H_0/J values at low temperatures in the

$(k_B T_c/J - H_0/J)$ plane. Further increase in p means a wider ferromagnetic region in the phase diagram, and finally for $p = 1.0$, the ferromagnetic region achieves its maximum size, and we recover the standard zero-field Ising model. Moreover, according to Fig. 6(b), as p increases, the area of the F + P region in the dynamic phase diagrams gets narrower, and after a specific value of p , we cannot observe any coexistence region in the $(k_B T_c/J - H_0/J)$ plane.

Variation of DOP (Q) as a function of the amplitude of the oscillating field H_0/J for a trimodal distribution corresponding to the dynamic phase diagrams depicted in Fig. 6 is plotted in Fig. 7 with some selected values of p . In this figure, the initial value of the average magnetization is selected as $m_0 = 0.0$. According to Fig. 7, DOP curves undergo first- and second-order dynamic phase transitions at low and high temperatures, respectively. At low temperatures, the critical amplitude value H_0^c/J at which a dynamic phase transition occurs depends on the initial magnetization m_0 . Namely, for $m_0 = 0.0$, the critical H_0^c/J value is greater than that obtained for $m_0 = 1.0$, which is due to the presence of the F + P phase in the system at a fixed value of p [see Fig. 6(b)].

Finally, for a fixed oscillation frequency $\omega = 0.5$, let us investigate the time dependence of the average magnetization $m(t)$ corresponding to the phase diagrams shown in Fig. 6(b). In Figs. 8(a) and 8(b), we plot the time series of $m(t)$ curves for $p = 0$, $k_B T/J = 1.0$, and with two values of field amplitude $H_0/J = 4.4$ and 4.58 , respectively. From Fig. 8(a), we see that the dynamic nature of the stationary state of the system is independent of the initial magnetization m_0 for $H_0/J = 4.4$. Namely, for this set of system parameters, the average magnetization of the system oscillates around a nonzero value (F phase) after some transient time. However, as shown in Fig. 8(b), for $H_0/J = 4.58$ (while the other parameters are the same), the stationary state of the system (F or P) depends on the initial magnetization m_0 , which indicates that the dynamic phase diagrams exhibit a coexistence region (F + P phase) in the $(k_B T_c/J - H_0/J)$ plane. On the other hand, as seen in Figs. 8(c) and 8(d), which are plotted for $p = 0.15$, we cannot observe any coexistent phase region in the system. Namely, for $H_0/J = 5.1$ with $k_B T/J = 1.0$, $m(t)$ curves oscillate around a finite nonzero value, whereas for $H_0/J = 5.22$ and $k_B T/J = 0.25$ the curves oscillate around zero, which means that the

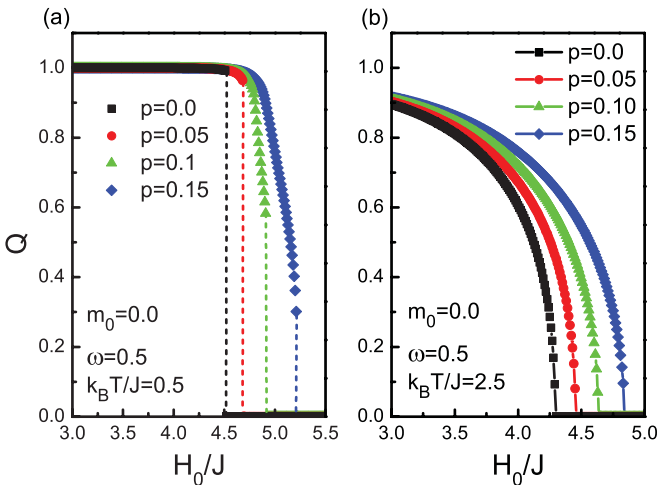


FIG. 7. (Color online) Variation of dynamic order parameter Q as a function of the amplitude of the oscillating field H_0/J for a trimodal distribution corresponding to the dynamic phase diagrams depicted in Fig. 6 with some selected values of p for $m_0 = 0$, $\omega = 0.5$, and for the reduced temperatures (a) $k_B T/J = 0.5$, (b) $k_B T/J = 2.5$.

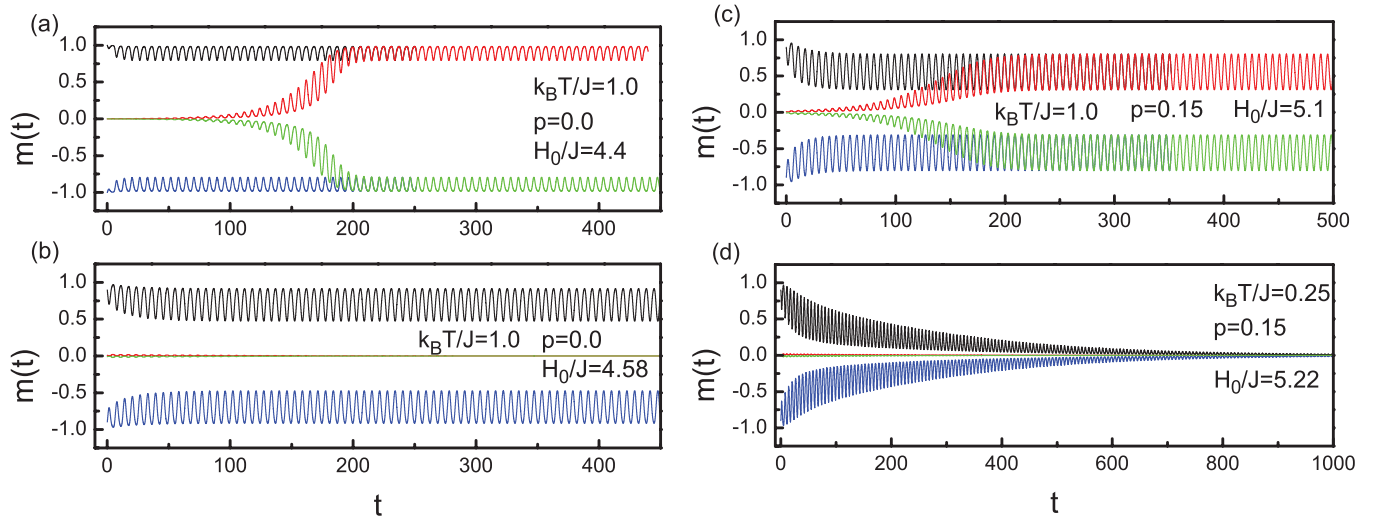


FIG. 8. (Color online) Time dependence of the average magnetization $m(t)$ for $\omega = 0.5$ with some selected values of the parameters. Left panel: $k_B T/J = 1.0$, $p = 0.0$, and (a) $H_0/J = 4.4$; (b) $H_0/J = 4.58$. Right panel: $p = 0.15$ with (c) $k_B T/J = 1.0$, $H_0/J = 5.1$; (d) $k_B T/J = 0.25$, $H_0/J = 5.22$.

system is in the P phase. Hence, we see that the stationary state of the system for a trimodal distribution of the oscillating field amplitude may be independent of m_0 , depending on the value of distribution parameter p .

IV. CONCLUDING REMARKS

In conclusion, we have investigated the kinetic behavior of a spin-1/2 Ising model on a simple cubic lattice ($q = 6$) under the influence of a quenched random magnetic field which oscillates periodically in time by means of an effective-field theory based on a standard decoupling approximation, and the time evolution of the system has been presented by utilizing a Glauber-type stochastic process. For bimodal and trimodal field distributions, we have studied the global dynamic phase diagrams of the system in a $(k_B T_c/J - H_0/J)$ plane and variation of the dynamic order parameter with respect to the temperature and random amplitude of the oscillating field, as well as the time series of the average magnetization curves. We found that the dynamic behavior of the random-field Ising model with a periodically oscillating magnetic field exhibits quite different characteristics in comparison with the static RFIM problem.

Our numerical analysis clearly indicates that such field distributions result in topologically different dynamic phase diagrams and may lead to a number of interesting phenomena. For example, we have found that for a bimodal distribution with sufficiently high frequency values, DOP curves, and nonequilibrium phase diagrams of the system resemble those of the pure kinetic Ising model driven by a periodic external field with the high oscillation frequency. On the other hand, we have also observed that F + P regions in $(k_B T_c/J - H_0/J)$ phase diagrams always exist for the whole range of frequency values for a bimodal distribution of oscillatory field amplitude, whereas for a trimodal distribution, the area of the F + P region gets narrower with increasing distribution parameter p , and if we increase p further, then we cannot observe any coexistence region in the $(k_B T_c/J - H_0/J)$ plane. One of the

main conclusions of the present work is that the dynamic phase transitions occurring between F (or P) and F + P phases in the $(k_B T_c/J - H_0/J)$ plane are found to be of first order, which signals the existence of a dynamic tricritical point. However, the nature of the transition (continuous or discontinuous) and the existence of the DTC point in the kinetic Ising model have been questioned throughout the years [42,46–48], and the situation also persists for the dynamic phase-transition properties of disordered systems, especially for the kinetic RFIM [54,56,57]. Hence, even according to the results based on some powerful methods such as MC simulations, in which one explicitly consider the thermal fluctuations, there is a controversy over whether kinetic RFIM exhibits a DTC point or not. In addition, the F + P phase region, which is quite clearly observed in conventional MFT predictions, gets rather narrower in EFT calculations [50], which is due to the fact that the EFT method takes the standard mean-field predictions one step forward by taking into account the single-site correlations, which means that the thermal fluctuations are partially considered within the framework of EFT.

Although all of the observations reported in this work show that EFT can be successfully applied to such nonequilibrium systems in the presence of quenched disorder, the true nature of the physical facts underlying the observations displayed in the system (especially the origin of the coexistence phase) may be further understood with an improved version of the present EFT formalism, which can be achieved by attempting to consider the multisite correlations that originate when expanding the spin identities. Such a method has been introduced by some of us [27] for the static RFIM problem. Therefore, the generalization of that work to the kinetic RFIM problem with a more general type of random fields, such as continuous disorder distributions, could resolve those specific questions mentioned above. In this context, we believe that this attempt could provide a treatment beyond the present approximation, and the results obtained in the present work would help to shed some light on the critical properties of the system.

ACKNOWLEDGMENTS

One of the authors (Y.Y.) would like to thank the Scientific and Technological Research Council of Turkey (TÜBİTAK) for partial financial support. The numerical calculations

reported in this paper were performed at TÜBİTAK ULAK-BİM, High Performance and Grid Computing Center (TR-Grid e-Infrastructure).

-
- [1] A. I. Larkin, *Sov. Phys. JETP* **31**, 784 (1970).
 [2] Y. Imry and S. K. Ma, *Phys. Rev. Lett.* **35**, 1399 (1975).
 [3] G. Grinstein and S. K. Ma, *Phys. Rev. Lett.* **49**, 685 (1982).
 [4] J. F. Fernandez, G. Grinstein, Y. Imry, and S. Kirkpatrick, *Phys. Rev. Lett.* **51**, 203 (1983).
 [5] J. Z. Imbrie, *Phys. Rev. Lett.* **53**, 1747 (1984).
 [6] J. Brimont and A. Kupiainen, *Phys. Rev. Lett.* **59**, 1829 (1987).
 [7] G. Parisi and N. Sourlas, *Phys. Rev. Lett.* **43**, 744 (1979).
 [8] K. Binder, Y. Imry, and E. Pytte, *Phys. Rev. B* **24**, 6736 (1981).
 [9] E. Pytte, Y. Imry, and D. Mukamel, *Phys. Rev. Lett.* **46**, 1173 (1981).
 [10] D. Mukamel and E. Pytte, *Phys. Rev. B* **25**, 4779 (1982).
 [11] A. Niemi, *Phys. Rev. Lett.* **49**, 1808 (1982).
 [12] D. P. Belanger, A. R. King, and V. Jaccarino, *Phys. Rev. B* **31**, 4538 (1985).
 [13] A. R. King, V. Jaccarino, D. P. Belanger, and S. M. Rezende, *Phys. Rev. B* **32**, 503 (1985).
 [14] I. B. Ferreira, A. R. King, V. Jaccarino, J. L. Cardy, and H. J. Guggenheim, *Phys. Rev. B* **28**, 5192 (1983).
 [15] H. Yoshizawa, R. A. Cowley, G. Shirane, R. J. Birgeneau, H. J. Guggenheim, and H. Ikeda, *Phys. Rev. Lett.* **48**, 438 (1982).
 [16] S. Fishman and A. Aharony, *J. Phys. C* **12**, L729 (1979).
 [17] J. L. Cardy, *Phys. Rev. B* **29**, 505 (1984).
 [18] T. Schneider and E. Pytte, *Phys. Rev. B* **15**, 1519 (1977).
 [19] D. Andelman, *Phys. Rev. B* **27**, 3079 (1983).
 [20] A. Aharony, *Phys. Rev. B* **18**, 3318 (1978).
 [21] D. C. Mattis, *Phys. Rev. Lett.* **55**, 3009 (1985).
 [22] M. Kaufman, P. E. Klunzinger, and A. Khurana, *Phys. Rev. B* **34**, 4766 (1986).
 [23] H. E. Borges and P. R. Silva, *Physica A* **144**, 561 (1987).
 [24] E. F. Sarmiento and T. Kaneyoshi, *Phys. Rev. B* **39**, 9555 (1989).
 [25] R. M. Sebastianes and W. Figueiredo, *Phys. Rev. B* **46**, 969 (1992).
 [26] T. Kaneyoshi, *Physica A* **139**, 455 (1985).
 [27] Ü. Akıncı, Y. Yüksel, and H. Polat, *Phys. Rev. E* **83**, 061103 (2011).
 [28] D. P. Landau, H. H. Lee, and W. Kao, *J. Appl. Phys.* **49**, 1356 (1978).
 [29] J. Machta, M. E. J. Newman, and L. B. Chayes, *Phys. Rev. E* **62**, 8782 (2000).
 [30] N. G. Fytas, A. Malakis, and K. Eftaxias, *J. Stat. Mech. Theory Exp.* (2008) P03015.
 [31] N. G. Fytas and A. Malakis, *Eur. Phys. J. B* **61**, 111 (2008).
 [32] M. Gofman, J. Adler, A. Aharony, A. B. Harris, and M. Schwartz, *Phys. Rev. B* **53**, 6362 (1996).
 [33] N. Crokidakis and F. D. Nobre, *J. Phys.: Condens. Matter* **20**, 145211 (2008).
 [34] O. R. Salmon, N. Crokidakis, and F. D. Nobre, *J. Phys.: Condens. Matter* **21**, 056005 (2009).
 [35] J.-C. Anglès D'Auriac and N. Sourlas, *Europhys. Lett.* **39**, 473 (1997).
 [36] D. Dhar, P. Shukla, and J. P. Sethna, *J. Phys. A* **30**, 5259 (1997).
 [37] A. K. Hartmann and U. Nowak, *Eur. Phys. J. B* **7**, 105 (1999).
 [38] Y. Wu and J. Machta, *Phys. Rev. B* **74**, 064418 (2006), and references therein.
 [39] B. K. Chakrabarti and M. Acharyya, *Rev. Mod. Phys.* **71**, 847 (1999), and references therein.
 [40] T. Tomé and M. J. de Oliveira, *Phys. Rev. A* **41**, 4251 (1990).
 [41] W. S. Lo and R. A. Pelcovits, *Phys. Rev. A* **42**, 7471 (1990).
 [42] M. Acharyya and B. K. Chakrabarti, *Phys. Rev. B* **52**, 6550 (1995).
 [43] M. Acharyya, *Physica A* **235**, 469 (1997).
 [44] M. Acharyya, *Phys. Rev. E* **56**, 2407 (1997).
 [45] M. Acharyya, *Phys. Rev. E* **58**, 179 (1998).
 [46] S. W. Sides, P. A. Rikvold, and M. A. Novotny, *Phys. Rev. Lett.* **81**, 834 (1998).
 [47] M. Acharyya, *Phys. Rev. E* **59**, 218 (1999).
 [48] G. Korniss, P. A. Rikvold, and M. A. Novotny, *Phys. Rev. E* **66**, 056127 (2002).
 [49] X. Shi, G. Wei, and L. Li, *Phys. Lett. A* **372**, 5922 (2008).
 [50] T. Kinoshita, S. Fujiyama, M. Tokita, and T. Idogaki, *J. Phys.: Conf. Ser.* **150**, 042091 (2009).
 [51] B. Deviren, O. Canko, and M. Keskin, *Chin. Phys. B* **19**, 050518 (2010).
 [52] Q. Jiang, H. N. Yang, and G. C. Wang, *Phys. Rev. B* **52**, 14911 (1995).
 [53] D. T. Robb, Y. H. Xu, O. Hellwig, J. McCord, A. Berger, M. A. Novotny, and P. A. Rikvold, *Phys. Rev. B* **78**, 134422 (2008).
 [54] J. Hausmann and P. Ruján, *Phys. Rev. Lett.* **79**, 3339 (1997).
 [55] G. L. S. Paula and W. Figueiredo, *Eur. Phys. J. B* **1**, 519 (1998).
 [56] M. Acharyya, *Phys. Rev. E* **58**, 174 (1998).
 [57] N. Crokidakis, *Phys. Rev. E* **81**, 041138 (2010).
 [58] E. Costabile and J. R. de Sousa, *Phys. Rev. E* **85**, 011121 (2012).
 [59] R. J. Glauber, *J. Math. Phys.* **4**, 294 (1963).
 [60] R. Honmura and T. Kaneyoshi, *J. Phys. C* **12**, 3979 (1979).
 [61] T. Kaneyoshi, *Acta Phys. Pol. A* **83**, 703 (1993).
 [62] I. Tamura and T. Kaneyoshi, *Prog. Theor. Phys.* **66**, 1892 (1981).